THE JOURNAL OF BIOLOGICAL CHEMISTRY VOL. 284, NO. 34, pp. 23083–23093, August 21, 2009

Characterization of Phospholipase Cγ Enzymes with Gain-of-Function Mutations*[S]

Received for publication, May 11, 2009, and in revised form, June 12, 2009 Published, JBC Papers in Press, June 16, 2009, DOI 10.1074/jbc.M109.019265

Katy L. Everett[‡], Tom D. Bunney[‡], Youngdae Yoon[§], Fernando Rodrigues-Lima[¶], Richard Harris[‖], Paul C. Driscoll[‖], Koichiro Abe[‡‡§§], Helmut Fuchs[‡‡], Martin Hrabé de Angelis[‡‡¶¶], Philipp Yu[‖‖], Wohnwa Cho[§], and Matilda Katan[‡1]**

*From the [‡]Section of Cell and Molecular Biology, Chester Beatty Laboratories, The Institute of Cancer Research, London SW3 6JB, United Kingdom, the [§]Department of Chemistry, University of Illinois at Chicago, Chicago, Illinois 60607-7061, the [¶]Unité de Biologie Fonctionnelle et Adaptative (BFA), CNRS EAC 7059, Laboratoire des Réponses Moléculaires et Cellulaires aux Xénobiotiques, Université Paris Diderot-Paris 7, 75013 Paris, France, the [‖]Division of Bioscience, Institute of Structural and Molecular Biology, University College London, London WC1E 6BT, United Kingdom, the **Division of Molecular Structure, Medical Research Council (MRC) National Institute for Medical Research, London NW7 1AA, United Kingdom, the [‡‡]Helmholtz Zentrum München, German Research Center for Environmental Health, Institute of Experimental Genetics, D-85764 Munich/Neuherberg, Germany, the [¶¶]Lehrstuhl für Experimentelle Genetik, Technische Universität München, D-85350 Freising-Weihenstephan, Germany, the [§§]Division of Basic Medical Science and Molecular Medicine, Tokai University School of Medicine, 259-1193 Kanagawa, Japan, and the [‖‖]Institute for Immunology, Philipps-Universität Marburg, 35032 Marburg, Germany*

Phospholipase Cγ isozymes (PLCγ1 and PLCγ2) have a crucial role in the regulation of a variety of cellular functions. Both enzymes have also been implicated in signaling events underlying aberrant cellular responses. Using *N*-ethyl-*N*-nitrosourea (ENU) mutagenesis, we have recently identified single point mutations in murine PLCγ2 that lead to spontaneous inflammation and autoimmunity. Here we describe further, mechanistic characterization of two gain-of-function mutations, D993G and Y495C, designated as ALI5 and ALI14. The residue Asp-993, mutated in ALI5, is a conserved residue in the catalytic domain of PLC enzymes. Analysis of PLCγ1 and PLCγ2 with point mutations of this residue showed that removal of the negative charge enhanced PLC activity in response to EGF stimulation or activation by Rac. Measurements of PLC activity *in vitro* and analysis of membrane binding have suggested that ALI5-type mutations facilitate membrane interactions without compromising substrate binding and hydrolysis. The residue mutated in ALI14 (Tyr-495) is within the spPH domain. Replacement of this residue had no effect on folding of the domain and enhanced Rac activation of PLCγ2 without increasing Rac binding. Importantly, the activation of the ALI14-PLCγ2 and corresponding PLCγ1 variants was enhanced in response to EGF stimulation and bypassed the requirement for phosphorylation of critical tyrosine residues. ALI5- and ALI14-type mutations affected basal activity only slightly; however, their combination resulted in a constitutively active PLC. Based on these data, we suggest that each mutation could compromise auto-inhibition in the inactive PLC, facilitating the activation process; in addition, ALI5-type mutations could enhance membrane interaction in the activated state.

Phosphoinositide-specific phospholipase C (PLC)[2] enzymes, comprising several families (PLCβ, γ, δ, ϵ, η, and ζ), have been established as crucial signaling molecules involved in regulation of a variety of cellular functions (1–4). PLC-catalyzed formation of the second messengers, inositol 1,4,5-trisphosphate (IP_3) and diacylglycerol, from phosphatidylinositol 4,5-bisphosphate (PIP_2), constitutes one of the major cell signaling responses. These second messengers provide a common link from highly specific receptors for hormones, neurotransmitters, antigens, and growth factors to downstream, intracellular targets; thus, they contribute to regulation of biological functions as diverse as cell motility, fertilization, and sensory transduction. Despite this central role for PLC enzymes in signaling networks, the molecular details of their regulation and possible subversion of these regulatory mechanisms in disease remain poorly understood.

Of two PLCγ enzymes, PLCγ1 is ubiquitously expressed and appears to regulate a multitude of cellular functions in many tissues. *Plcg1*-null mice die by embryonic day 9, highlighting the widespread importance of this enzyme (5). PLCγ1 is activated in response to growth factor stimulation; in addition, its function in T-cell responses has been extensively documented (1). PLCγ2, in contrast, is most highly expressed in cells of the hematopoietic system and plays a key role in regulation of the immune response. Consistent with this, *Plcg2*-null mice display defects in the functioning of B cells, platelets, mast cells, and natural killer cells (6).

Both PLCγ enzymes have also been implicated in signaling events underlying aberrant cellular responses. PLCγ1 is critically involved in the regulation of cancer cell motility (7–11) while PLCγ2 has been implicated in deregulation of the immune responses resembling Btk-dependent X-linked agammaglobulinaemia and SLE disease in humans (12–14). It has been suggested that, in cancer cells, PLCγ1 could function as a

* This work was supported in part by Cancer Research UK (to M. K.), the Association pour la Recherche sur le Cancer (ARC) and Association Française contre les Myopathies (AFM) (to F. R. L.), and the MRC (to K. L. E.).

[S] The on-line version of this article (available at http://www.jbc.org) contains supplemental Figs. S1–S3 and Methods.

[1] To whom correspondence should be addressed. E-mail: matilda.katan@icr.ac.uk.

[2] The abbreviations used are: PLCγ, phospholipase Cγ; ENU, *N*-ethyl-*N*-nitrosourea; DMEM, Dulbecco's modified Eagle's medium; BCR, B-cell receptor; EGF, epidermal growth factor; IP_3, inositol 1,4,5-trisphosphate; PIP_2, phosphatidylinositol 4,5-bisphosphate.

key, rate-limiting, common component involved in cell motility triggered by several growth factors and integrins (7). In some cancer cells, this increased motility could result from deregulation *i.e.* higher levels of expression of PLCγ1 (15, 16). The possibility that the activity of PLCγ could be up-regulated due to mutation has not yet been fully investigated in cancer. Previous studies of PLCγ2, however, have demonstrated the first gain-of-function mutation in a PLC molecule in the context of an organism, and shown that, in principle, PLC activity can be greatly enhanced by point mutations (13). Furthermore, this work has demonstrated that such a mutation is linked to a dramatic phenotypic disorder. By using a large scale ENU mutagenesis to discover new immune regulators, several mouse strains were generated with spontaneous autoimmune and inflammatory symptoms; two of these strains harbor a mutation in PLCγ2. In addition to the previously described ALI5 mutation (13) the ALI14 mutation has been identified very recently.[3] Strikingly, the well-characterized ALI5 phenotype has shown that the mutation affects many cellular functions deregulated in *Plcg2*-null mice. Notably, while in *Plcg2*-null mice such responses are lacking, the ALI5 mutation resulted in their enhancement. In particular, further analyses of the ALI5 mutation in the context of signaling in B-cells have demonstrated that calcium responses to the crosslinking of the B-cell receptor were enhanced and prolonged resulting in enhanced deletion of B cells and autoreactivity (13).

The domain organization of PLCγ enzymes is characterized by the insertion of a highly structured region (PLCγ-specific array, γSA) between the two halves of the TIM-barrel catalytic domain common to all PLCs. The γSA comprises a split PH (spPH) domain flanking two tandem SH2 domains and a SH3 domain (1). A distinct regulatory feature of PLCγ enzymes is that their activation is linked to an increase in phosphorylation of specific tyrosine residues (most notably within the γSA) by receptor and non-receptor tyrosine kinases (17, 18). Furthermore, multiple protein-protein interactions (mainly mediated by SH2 domains) also contribute to activation and have an important role in localizing PLCγ into protein complexes with different binding partners, depending on cell type and specific cellular compartments. One mode of activation that is specific for the PLCγ2 isozyme is direct binding to and activation by Rac. The interaction involves the spPH domain, and this activation mechanism does not require tyrosine phosphorylation (19, 20). In molecular terms, changes that lead to PLC activation in response to different input signals, or due to point mutations, are not well understood and require further studies.

Here we describe further analysis of the two gain-of-function mutations, ALI5 and ALI14, obtained using ENU mutagenesis. These mutations map to different regions in PLCγ2, and we performed detailed analysis of these regions in both PLCγ isozymes. To characterize the molecular mechanism of gain-of-function, we combined studies *in vitro* and in different cellular signaling contexts. We have found that ALI5- and ALI14-type point mutations lead, by distinct mechanisms, to an enhancement of responses to a variety of input signals while their combination results in a constitutively active PLC enzyme.

EXPERIMENTAL PROCEDURES

Materials—PLCγ1 antibody (P8104) was purchased from Sigma. PLCγ2 (sc-407) and Rac2 (sc-96) antibodies were purchased from Santa Cruz Biotechnology. GAPDH antibody (10R-G109a) was purchased from Fitzgerald. Penta-His antibody (38660) was purchased from Qiagen. Phosphotyrosine antibody (PY20) was purchased from BD Transduction Laboratories. 1-Palmitoyl-2-oleoyl-*sn*-glycero-3-phosphocholine (POPC), 1-palmitoyl-2-oleoyl-*sn*-glycero-3-phosphoethanolamine (POPE), 1-palmitoyl-2-oleoyl-*sn*-glycero-3-phosphoserine (POPS), and cholesterol were purchased from Avanti Polar Lipids. 1,2-dipalmitoyl derivatives of phosphatidylinositol-(4,5)-bisphosphate (PIP_2), phosphatidylinositol-(3,4,5)-trisphosphate (PIP_3), and phosphatidylinositol were from Cayman Chemical. For the activity measurements L-α-PIP_2 was purchased from Sigma and PIP_2 [inositol 2-^{3}H (N)] from PerkinElmer Life Sciences.

Abnormal Limb 14 (ALI14) Mutant Mouse Strain—The *Ali14* mutation was generated in a large scale *N*-ethyl-*N*-nitrosourea (ENU) mouse mutagenesis program (21). The first ALI14 mutant mouse was identified in the dominant dysmorphology screen (22) based on a phenotype marked by swollen footpads due to inflammation. The mutation has been stably maintained on the original C3HeB/FeJ genetic background through more than 20 backcrosses to the wild type. Detailed analysis of the phenotype, genetic mapping, and mutation detection of *Ali14* have been performed using the same methodology as for ALI5 mice (13) and is being described elsewhere.[4]

Construction of Vectors—cDNA encoding bovine PLCγ1 and human PLCγ2 were inserted into pTriEx-4 (Novagen). pcDNA3.1(+) $Rac2^{G12V}$ construct was described in (20). Human PLCγ1 encoding residues 3–1224 was inserted into pDest10 (Invitrogen) using Gateway® Technology. This construct was used to produce baculoviruses. QuikChange PCR mutagenesis (Stratagene) was used to introduce point mutations. All mutants were fully sequenced to verify the fidelity of PCR.

Cell Culture and Transfection—COS-7 cells were maintained at 37 °C in a humidified atmosphere of 95% air and 5% CO_2 in Dulbecco's modified Eagle's medium (DMEM) (Invitrogen) supplemented with 10% (v/v) fetal bovine serum (Invitrogen) and 2.5 mM glutamine. Prior to transfection cells were seeded into 6-well plates at a density of 2.5×10^5 cells/well and grown for 16 h in 2 ml/well of the same medium. For transfection, 1.0 μg of PLCγ DNA was mixed with 1 μl of PlusReagent™ and 7 μl of Lipofectamine™ (Invitrogen) and added to the cells in 0.8 ml of DMEM without serum. The cells were incubated for 3.5 h at 37 °C, 5% CO_2 before the transfection mixture was removed and replaced with DMEM-containing serum.

Analysis of Inositol Phosphate Formation in Intact COS-7 Cells—24 h after transfection, the cells were washed twice with inositol-free DMEM without serum and incubated for 24 h in 1.5 ml of the same medium supplemented with 0.25% fatty acid free bovine serum albumin (Sigma) and 1.5 μCi/ml myo-[2-

[3] K. Abe, H. Fuchs, and M. Hrabé de Angelis, unpublished data.

[4] K. Abe, H. Fuchs, and M. Hrabé de Angelis, manuscript in preparation.

^{3}H]inositol (MP Biomedicals). After a further 24 h, the cells were incubated in 1.2 ml of inositol-free DMEM without serum containing 20 mM LiCl with or without stimulation with 100 ng/ml EGF (Calbiochem). The cells were lysed by addition of 1.2 ml of 4.5% perchloric acid. After incubating the samples on ice for 30 min, they were centrifuged for 20 min at 3700 × *g*. Supernatants and pellets were separated.

The supernatants were neutralized by addition of 3 ml of 0.5 M potassium hydroxide/9 mM sodium tetraborate and centrifuged for a further 20 min at 3700 × *g*. Supernatants were loaded onto AG1-X8 200–400 columns (Bio-Rad) that had been converted to the formate form by addition of 2 M ammonium formate/0.1 M formic acid and equilibrated with water. The columns were washed three times with 5 ml of 60 mM ammonium formate/5 mM sodium tetraborate, and inositol phosphates were eluted with 5 ml of 1.2 M ammonium formate/0.1 M formic acid. 5 ml Ultima-Flo scintillation fluid (PerkinElmer Life Sciences) was added to the eluates and the radioactivity quantified by liquid scintillation counting. The values represent total inositol phosphates.

The pellets from the first centrifugation were resuspended in 100 μl of water and 375 μl of chloroform/methanol/HCl (200:100:15) was added. The samples were vortexed, and an additional 125 μl of chloroform and 125 μl of 0.1 M HCl were added. After further vortexing, the samples were centrifuged at 700 × *g* for 10 min. 10 μl of the lower phase were placed in a scintillation vial with 3 ml of Ultima-Flo scintillation fluid and the radioactivity quantified by liquid scintillation counting. The obtained values correspond to radioactivity in inositol lipids.

PLC activity is expressed as the total inositol phosphates formed relative to the amount of [^{3}H]myo-inositol in the phospholipid pool. Because the differences in steady state labeling of inositol lipids are small (within 20%), this normalized PLC activity corresponds closely to PLC values expressed as total inositol phosphates; however, the error bars between the duplicates are generally smaller.

Expression and Purification of Proteins—For production of recombinant PLCγ1 (3–1224) (wild type and mutants), baculovirus-infected Sf9 cells were grown in suspension culture in Sf-900 II SFM medium (Invitrogen) in 2000-ml roller bottles. Cells were infected with baculovirus at 1.8 × 10^6 cell/ml in a 400-ml culture and incubated for 72 h at 27 °C on a rotary shaker at 140 rpm. Cells were harvested by centrifugation at 2000 × *g* for 15 min and then snap-frozen in liquid nitrogen. Pellets were stored at −80 °C until required.

Frozen pellets were lysed with 20 ml of lysis buffer (50 mM Tris/Cl, 400 mM NaCl, 1 mM $MgCl_2$ 1% Triton X-100, 1 mM TCEP, 1 mM AEBSF, 1× Complete EDTA-free protease inhibitor mixture (Roche Applied Science), 400 units of DNaseI, pH 8.0) at 4 °C on a rotating wheel for 1 h. The lysate was centrifuged at 17,500 × *g* for 1 h, and the recombinant protein was then purified by a five step process. First, the supernatant was loaded onto a 5 ml of HisTrap column (GE Healthcare) with wash buffer A (25 mM Tris/Cl, 500 mM NaCl, 40 mM imidazole, and 1 mM tris(2-carboxyethyl)phosphine (TCEP), pH 8.0) and eluted with elution buffer B (25 mM Tris/Cl, 500 mM NaCl, 500 mM imidazole, and 1 mM TCEP, pH 8.0). Second, the purification tags were proteolytically cleaved overnight by TeV protease in cleavage and dialysis buffer C (25 mM Tris/Cl, 150 mM NaCl, 10 mM imidazole, and 1 mM TCEP, pH 8.0) at 4 °C. Third, the cleaved protein was passed over a Ni^{2+}-loaded HiTrap chelating column (GE Healthcare) in buffer C and the flow-through collected. Fourth, the flow-through fraction was loaded on a Superdex 200 26/60 gel filtration column (GE Healthcare) in gel filtration buffer D (25 mM Tris/Cl, 50 mM NaCl, and 1 mM TCEP, pH 8.0) and fractions of monomeric protein collected. Finally, these fractions were concentrated by loading on a 1-ml Resource Q column (GE Healthcare) in wash buffer E (20 mM Tris/Cl and 1 mM TCEP, pH 8.0) and elution on a NaCl gradient with elution buffer F (20 mM Tris/Cl, 1 M NaCl and 1 mM TCEP, pH 8.0). Fractions containing concentrated protein were snap-frozen and stored at −80 °C.

PLC Activity in Mixed Micelles—The assay was based on the method described in Ellis *et al.* (23). The reaction contained 20 mM Tris/Cl pH 6.8, 0.4 mg/ml bovine serum albumin, 5 mM 2-mercaptoethanol, 4 mM EGTA, 2 mM $CaCl_2$, 100 mM NaCl, 0.4% sodium cholate, 200 μM PIP_2, and 25 ng of protein in 50 μl. Reactions were incubated at 37 °C for 20 min.

NMR Spectroscopy—The one-dimensional ^{1}H NMR spectrum of spPH proteins was obtained at 25 °C on a Varian UnityPLUS spectrometer (500 MHz) using pulse field gradient-based water suppression. Resonances were obtained from the backbone NH and aromatic side chain CH protons (20).

Isothermal Titration Calorimetry (ITC)—Heats of interaction were measured as described in Bunney *et al.* (24). Briefly, a MSC system (Microcal) with a cell volume of 1,458 ml was used. Proteins were loaded in the sample cell at 300 mM and titrated with the binding partner in the syringe (2 mM). The titrations were performed with stirring at 260 rpm, at 25 °C. The data were fitted with a single site model using Origin software (Microcal) (24).

Protein Modeling—Alignments of PLCδ1 with PLCγ1 and PLCγ2 were made with ClustalW and used in combination with the PLCδ1 structure (PDB:2ISD) to identify the X and Y region in the catalytic domains. The raw sequences of these regions from PLCγ1 and PLCγ2 were loaded in DeapView/Swiss-PDBViewer and three-dimensional models constructed using the SwissModel server (25). Side chains were repositioned in optimized conformations using SCWRL (26). Stereochemical verifications of the models were carried out using Procheck (27) and ProSA (28). The models were analyzed using DeapView/Swiss-PDBViewer and Pymol.

Surface Plasmon Resonance Measurements—All surface plasmon resonance measurements were performed at 23 °C using a lipid-coated L1 chip in the BIACORE X system as described previously (29). Briefly, after washing the sensor chip surface with the running buffer (50 mM Tris/Cl, pH 7.4, containing 0.16 M KCl), POPC/POPE/POPS/cholesterol/PIP_3 (12:33:22:8:22:3%) and POPC (100%) vesicles were injected at 5 ml/min to the active surface and the control surface, respectively, to give the same resonance unit (RU) values. The level of lipid coating for both surfaces was kept at the minimum that is necessary for preventing the nonspecific adsorption to the sensor chips. This low surface coverage minimized the mass transport effect and kept the total protein concentration above the total concentration of protein binding sites on vesicles. For

A

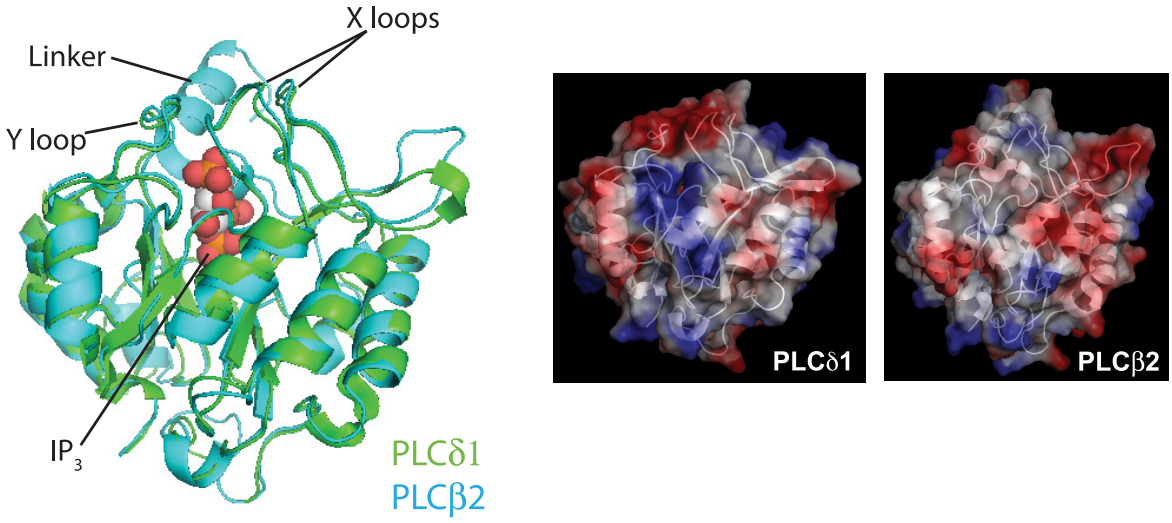

B

```
                          X Loop 1                                                X Loop 2
PLCδ1     QPLSHYLVSSSHNTYLLEDQLAGPSSTEAYIRALCKGCRCLELDCWDG--PNQEPIIYHGYTFTSKILFCDVLRAIRDYAFKASPYPVILSLENHCTLE
PLCβ2     QPLNHYFINSSHNTYLTAGQFSGLSSAEMYRQVLLSGCRCVELDCWKGKPPDEEPIITHGFTMTTDIFFKEAIEAIAESAFKTSPYPIILSFENHVDSP
PLCγ1     NPLSHYWISSSHNTYLTGDQFSSESSLEAYARCLRMGCRCIELDCWDG--PDGMPVIYHGHTLTTKIKFSDVLHTIKEHAFVASEYPVILSIEDHCSIA
PLCγ2     NPLSHYWISSSHNTYLTGDQLRSESSPEAYIRCLRMGCRCIELDCWDG--PDGKPVIYHGWTRTTKIKFDDVVQAIKDHAFVTSSFPVILSIEEHCSVE
          :**.** :.******  .*: . ** * * : *  ****:*****.*  *:  *:* ** * *:.* * :.:.:* : ** :* :*:***:*:*

                                                                 XY LINKER
PLCδ1     -QQRVMARHLHAILGPMLLNRPLDGVTNS----LPSPEQLKGKILLKGKKL..                  ..LAQELSDMVIYCKSVHFGGFSSPGTPGQAFYEM
PLCβ2     RQQAKMAEYCRTIFGDMLLTEPLEKFPLKPGVPLPSPEDLRGKILIKNKKN..                  ..AYEEMSSLVNYIQPTKFVSFEFS-AQKNRSYVI
PLCγ1     -QQRNMAQYFKKVLGDTLLTKPVEISADG----LPSPNQLKRKILIKHKKL..                  ..IALELSELVVYCRPVPFDEEKIG-TERACYRDM
PLCγ2     -QQRHMAKAFKEVFGDLLLTKPTEASADQ----LPSPSQLREKIIIKHKKL..                  ..IAIELSDLVVYCKPTSKTKDNLE---NPDFREI
           **  **.  : ::*  **.* :  .       ****.:*: **::* **                      *:*.:* * :..     .

                                  Y Loop
PLCδ1     ASFSENRALRLLQESG-NGFVRHNVGHLSRIYPAGWRTDSSNYSPVEMWNGGCQIVALNFQTPGPEMDVYQGRFQ
PLCβ2     SSFTELKAYDLLSKAS-VQFVDYNKRQMSRIYPKGTRMDSSNYMPQMFWNAGCQMVALNFQTMDLPMQQNMAVFE
PLCγ1     SSFPETKAEKYVNKAKGKKFLQYNRLQLSRIYPKGQRLDSSNYDPLPMWICGSQLVALNFQTPDKPMQMNQALFM
PLCγ2     RSFVETKADSIIRQKP-VDLLKYNQKGLTRVYPKGQRVDSSNYDPFRLWLCGSQMVALNFQTADKYMQMNHALFS
          :** * :*  : :     ::  :*   ::*:** * * ***** *  :*  *.*:******* .  *:   . *
```

C

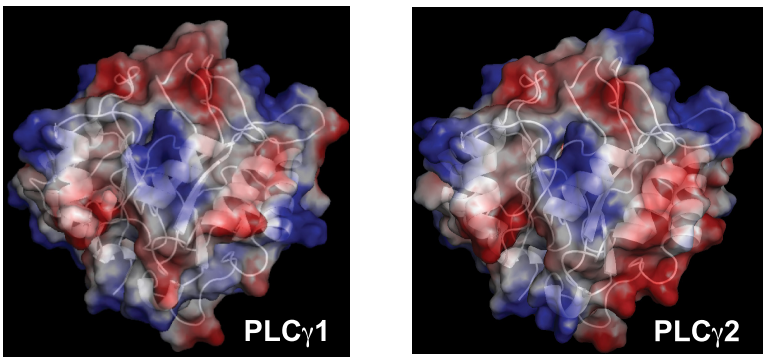

D

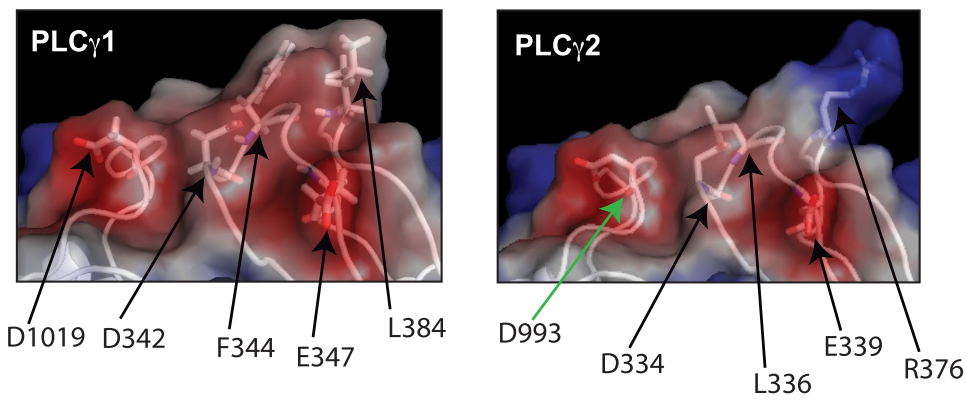

PLCγ1 lipid binding measurements, the flow rate was maintained at 15 ml/min for both association and dissociation phases.

RESULTS

ALI5 Mutation and the Ridge Region Surrounding the PLC Active Site—The PLCγ2 residue altered in ALI5 mice (Asp-993) has been mapped to the structurally defined catalytic domain (Fig. 1*A*) that has high sequence similarity between different PLC families (Fig. 1*B* and supplemental Fig. S1). The residue corresponding to Asp-993 in PLCγ2 is present in all PLC families (Fig. 1*B* and supplemental, Fig. S1). The two available structures of the catalytic domain from PLCδ1 and PLCβ2 superimpose well and provided a good template for modeling the catalytic domain from PLCγ enzymes. These models are shown in Fig. 1*C*. Residue Asp-993 and the corresponding Asp-1019 in PLCγ1 are present within one of 3 loops that form a ridge around the active site. The ridge region contains several negatively charged and hydrophobic residues. Residues Asp-1019, Asp-342, Phe-344, and Glu-347 in PLCγ1 correspond to Asp-993, Asp-334, Leu-336, and Glu-339 in PLCγ2, respectively (Fig. 1*D*).

The ALI5 mutation in PLCγ2, D993G, has been analyzed in the context of B-cell signaling, and the data showed an increase in IP_3 and calcium generation in stimulated cells in response to BCR activation (13). We first tested whether the impact of this mutation is restricted to B-cell components or has a more general impact on PLCγ2 activity. After transfection in COS cells, the PLCγ2 D993G variant has enhanced activation (about 6-fold) following EGF stimulation or co-transfection with the activated variant of Rac (Fig. 2, *A* and *B*). Subsequently, we analyzed the corresponding PLCγ1 mutation with respect to EGF-stimulated activation; this signaling context has been particularly well defined for the PLCγ1 isozyme. The effect of D1019G replacement was similar to the D993G mutation in PLCγ2, giving a severalfold enhancement of activity over the wild type (Fig. 2*D*).

Analysis of the Ridge Region in PLCγ Isozymes—We further tested whether enhanced PLC activation following replacement of Asp-993 or the corresponding Asp-1019 was a consequence of the removal of negative charge in this region or was due to a change in local conformation. As shown in Fig. 2*D*, the replacement of Asp-1019 by alanine, leucine or asparagine, like the ALI5 mutation (replacement by glycine), resulted in an enhanced activation in EGF-stimulated cells. The most striking activation was observed for the D1019L variant; here the leucine side chain has a similar size to aspartic acid but lacks the negative charge. These data suggest that in the wild-type PLC enzyme, the negative charge of the conserved Asp-1019 residue has a role in limiting PLC activity toward the substrate, presented within the overall negatively charged plasma membrane, and that the removal of this negative charge leads to gain-of-function. This conclusion was further supported by analysis of two other negatively charged residues in PLCγ1: Asp-342 and Glu-347. Replacement of these residues by glycine, alanine, leucine, or asparagine/glutamine, enhanced PLC activity in response to EGF and resulted in about 1.5–4 fold increase of PLC activity (supplemental Fig. S2, *A* and *B*). In contrast, replacement of hydrophobic residues within the ridge region resulted in reduced activity (Fig. 2*E* and supplemental Fig. S2*C*).

The ridge region could have a role in both binding of the lipid chains of the substrate PIP_2 and interaction with the surrounding membrane surface (23). The substrate binding and the membrane binding of PLC were separately measured by the detergent/PIP_2 mixed micelle assay and by surface plasmon resonance analysis, respectively. In the mixed micelle assay the ability to bind and hydrolyze PIP_2 is tested more directly than in a vesicle assay, because the effect of mutations on interaction with the membrane surface is typically much less in the former than in the latter (23). The removal of the acidic residue, D1019L, did not affect substrate hydrolysis in the mixed micelle assay (as was the case for the F344A variant) (Fig. 3*A*) but did enhance binding to the membrane measured by surface plasmon resonance (Fig. 3*B*). These data thus suggest that ALI5-type replacements lead to gain-of-function by increasing the interaction with the membrane surface without compromising substrate binding and hydrolysis.

ALI14 Gain-of-Function Mutation in the spPH Domain of PLCγ2—Using the same strategy that generated ALI5 mice, another strain with a gain-of-function, single point mutation mapping to the *Plcg2* locus has been identified and designated as ALI14.[3] The residue mutated in ALI14, Y495C, is not within the catalytic domain but within the spPH domain that is specific to the PLCγ family (Fig. 4*A*). Interestingly, this spPH domain in PLCγ2 has been identified as the binding site for the small GTPase Rac (20). Based on the structure of the spPH/Rac2 complex that we have solved recently (24), the mutation of residue Tyr-495 is not likely to affect this interaction directly. Tyr-495 is present in the β2-strand of the spPH domain and

FIGURE 1. **Structures and modeling of catalytic domains from PLC isoforms.** *A*, structural alignment of the catalytic domains of PLCδ1 (PDB:2DJX) and PLCβ2 (PDB:2ZKM) (*left panel*) shows that the TIM barrel is structurally well conserved even in many of the loop regions. Also highlighted is the IP_3 molecule from 2DJX, representing the position of the PIP_2 headgroup in the active site. The indicated linker between the two halves (X and Y) of the catalytic TIM-barrel domain was determined only in the PLCβ2 structure. The 3 loops in both PLCδ1 and PLCβ2 structures positioned in the vicinity of the active site are also indicated; two loops are from the X half (*X loops*) and one from the Y half (*Y loop*) of the TIM barrel. Surface charge maps generated with PyMol (*right panels*) indicate some differences between the domains. *B*, sequence alignment of the catalytic domains of human PLCδ1 (300–442, 488–594), PLCβ2 (316–465, 542–647), PLCγ1 (324–466, 949–1055), and PLCγ2 (316–458, 926–1029). *Red bars* indicate the three loops that form the ridge around the active site. The residue mutated in ALI5 mice is highlighted in *green*. Residues mutated in PLCγ1 are *underlined*. The *dashed box* indicates the position of variable X-Y linkers, which cannot be aligned, connecting the X and Y halves of the TIM barrel. *C*, models of the PLCγ1 and PLCγ2 catalytic domains were produced with SwissModel using the catalytic domain of PLCδ1 (PDB:2ISD) as the template. Using Procheck to check the stereochemical quality of the models showed that the number of residues in the favored regions of the Ramachandran plot was 98 and 97% for PLCγ1 and PLCγ2, respectively. Use of ProSA II showed that the overall model quality was similar to the quality of the template. PyMol was used to generate surface charge maps. *D*, based on the structural models, the ridge region around the active site of PLCγ1 and PLCγ2 was further analyzed by site-directed mutagenesis; the residues were chosen according to their location in the charged or hydrophobic areas of the ridge region. *Green arrow* indicates Asp-993 in PLCγ2 that is replaced by glycine in ALI5 mice.

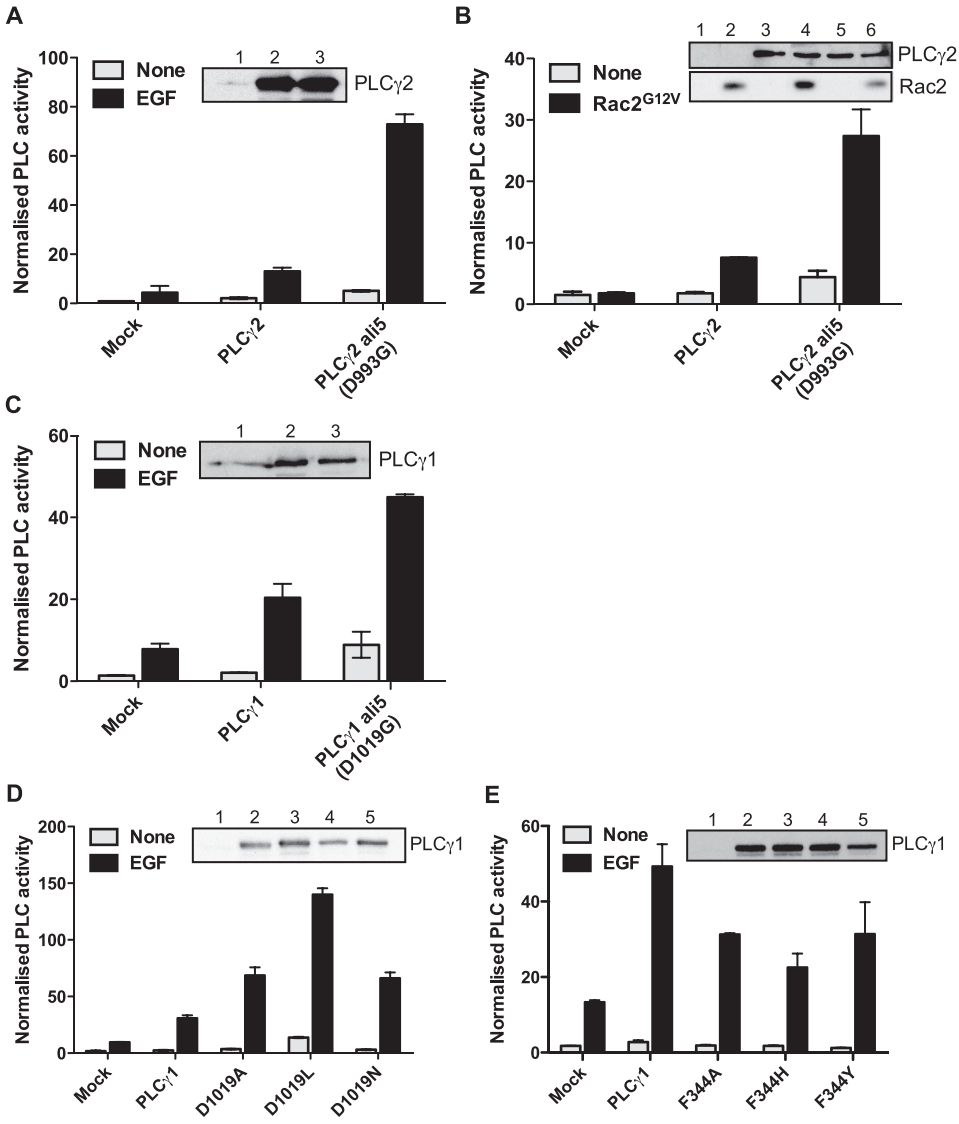

FIGURE 2. **Mutations in the ridge region affect PLC activity.** Inositol phosphate production was measured in COS-7 cells transiently transfected with the indicated variants of PLC isozymes: *A*, PLCγ2 wild type and ALI5 (D993G); *B*, PLCγ2 wild type and ALI5 co-transfected with $Rac2^{G12V}$; *C*, PLCγ1 wild type and PLCγ1 incorporating D1019G replacement corresponding to ALI5 in PLCγ2; *D*, PLCγ1 wild type and PLCγ1 with different mutants of Asp-1019; *E*, PLCγ1 wild type and PLCγ1 with different mutants of Phe-344. Cells were stimulated with 100 ng/ml EGF as indicated. For all experiments in COS cells, the amount of DNA used for transfection was adjusted to give comparable expression. Cells transfected in parallel but not radiolabeled were used for Western blotting (*insets*). *Lanes 1–3* in *A* correspond to mock (*1*), PLCγ2 wild type (*2*), and ALI5 (*3*). *Lanes 1–6* in *B* correspond to mock (*1*, *2*), PLCγ2 wild type (3, 4), and ALI5 (5, 6). *Lanes 1–3* in *C* correspond to mock (*1*), PLCγ1 wild type (*2*), and ALI5 (*3*). *Lanes 1–5* in *D* correspond to mock (*1*), PLCγ1 wild type (*2*), D1019A variant (*3*), D1019L variant (*4*), and D1019N variant (*5*). *Lanes 1–5* in *E* correspond to mock (*1*), PLCγ1 wild type (*2*), F344A variant (*3*), F344H variant (*4*), and F344Y variant (*5*). The data are representative for at least three independent experiments.

distant from the Rac binding surface that centers on the α-helix at the C terminus (Fig. 4*B*).

In our analysis of the Y495C mutation, we first analyzed whether this substitution affects folding of the spPH domain. Data obtained using one-dimensional NMR spectroscopy showed that this was not the case, because the spectra of the spPH Y495C variant and the wild type were comparable while the mutation of Trp-899, known to be structurally important, impaired folding (Fig. 4*C*). We also tested Rac2 binding by the wild-type spPH domain and variants incorporating mutations Y495C and W899A using ITC. This analysis has shown that the replacement of Tyr-495 did not have a marked effect on spPH/Rac2 interaction, as was the case for the Trp-899 variant; some reduction of binding was observed for the Y495C variant (Fig. 4*D*). Subsequently, we analyzed activation of the full-length PLCγ2 incorporating Y495C or Y495F mutation by Rac2 V12 after co-transfection in COS cells. Both the Y495C mutation (Fig. 4*E*) and the conservative substitution, Y495F (supplemental Fig. S3A) resulted in the enhanced activation of PLCγ2 compared with the wild type. Our additional experiments in COS cells suggested that Tyr-495 was not phosphorylated after EGF stimulation (supplemental Fig. 3*B*).

Together, the data in Fig. 4 show that the ALI14 mutation resulted in a gain-of-function when analyzed for activation by Rac in a COS cell assay. This enhanced activation however is not due to direct or indirect effects on the spPH/Rac interaction since Tyr-495 is not at the interaction surface and does not affect spPH domain folding or enhance Rac binding. The Tyr-495 mutation is therefore more likely to affect some other functions of spPH domain with more general impact on PLC regulation. To further test this possibility we extended our studies to include other agonists and also the Rac-insensitive PLCγ1 isozyme.

Analysis of the spPH Domain in PLCγ Isozymes—The structure of spPH domain from PLCγ1 has also been solved and despite relatively low sequence identity (29%), the spPH domain folds from PLCγ1 and PLCγ2 superimpose well (Fig. 5*A*, *left panel*). As we described in the previous section, the differences that are critical for specific Rac binding are within the α-helix and not in the β2-strand where the ALI14 mutation has been mapped. Tyr-509 in PLCγ1 corresponds to Tyr-495 in PLCγ2; however, the surrounding sequences are not highly conserved (Fig. 5*A*, *right panel*).

Interestingly, in a previous independent study of PLCγ1 in response to B-cell and T-cell stimulation measured by NFAT activation, the N-terminal part of the spPH domain has been identified as an important regulatory element (30). In particular, a more comprehensive analysis of this region identified a double mutation Y509A/F510A that greatly increased BCR-induced transcription of NFAT in P10–14 cells and resulted in prolonged calcium responses to agonist stimulation (30). Because

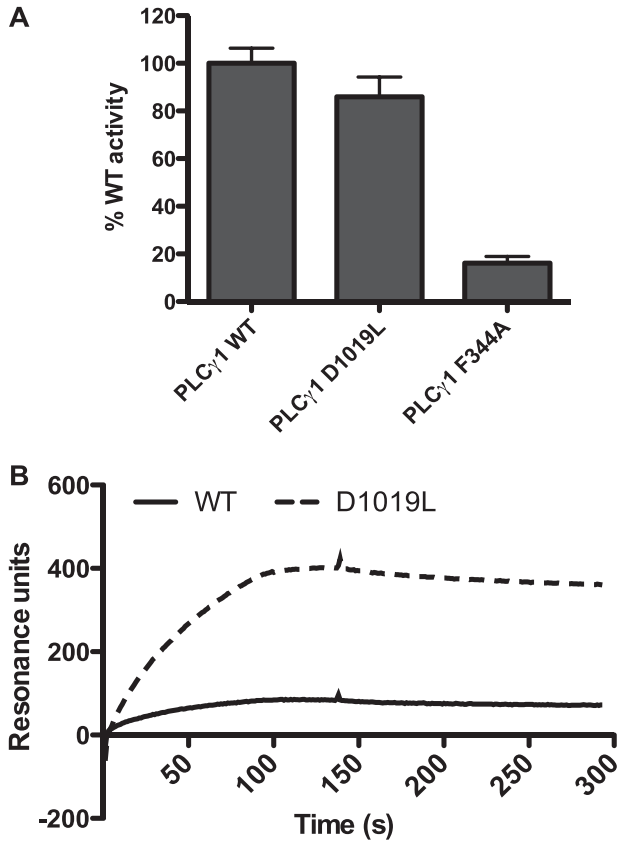

FIGURE 3. ***In vitro* studies of PLCγ1 ridge mutants.** *A*, PLC activity was analyzed *in vitro*, using purified recombinant protein and substrate presented as detergent/PIP_2 mixed micelles; this assay is different from the measurements of PLC activity in a cellular setting (COS-7 cells) shown in Figs. 2, 4, 5, and 6. PLC activity in this *in vitro* assay was measured as IP_3 production by PLCγ1 wild type and mutants using PIP_2 micelles formed in the presence of sodium cholate. 25 ng of recombinant protein, within the linear range of PLC activity, was used in each assay. *B*, surface plasmon resonance measurements were obtained for the binding of the PLCγ1 wild type and D1019L variants to a plasma membrane mimetic containing POPC/POPE/POPS/cholesterol/PIP_3 (12: 33: 22: 8: 22: 3%). PC binding was used as a control for nonspecific, background binding.

the residue Tyr-509 in PLCγ1 corresponds to Tyr-495 in PLCγ2 that is mutated in ALI14, we generated PLCγ1 variants that incorporate single point mutations Y509A and F510A and compared them to the double mutation Y509A/F510A in PLCγ1 and the ALI14 mutation in PLCγ2. For this analysis, PLCγ constructs were transfected into COS cells, and the cells subsequently stimulated with EGF. As shown in Fig. 5*B*, PLCγ2 ALI14 variant had the same enhanced responses to EGF as was observed with stimulation by Rac2. Similarly, all the PLCγ1 variants incorporating the specified mutations had greater responses to EGF compared with wild type (Fig. 5, *C* and *D*). This contrasts with several other conserved residues on the same surface of the spPH that showed no enhanced activity in response to EGF (supplemental Fig. S3, *C–E*). As expected from the location of the mutations in the spPH domain, ALI14-type mutations did not directly affect PIP_2 hydrolysis, when analyzed with mixed micelles *in vitro*, or the binding to phospholipids surfaces measured using surface plasmon resonance (data not shown).

Taken together, the data shown in Fig. 5 are consistent with the concept that, as is the case with ALI5, the ALI14 gain-of-function mutation affects some general features of basal regulatory mechanisms that when removed lead to greater responsiveness to a variety of upstream signals.

Effects of Combining Mutations in PLCγ Enzymes—Both ALI5- and ALI14-type mutations affected the level of PLCγ activity following stimulation; however, each mutation had only a very small effect on the basal PLC activity in non-stimulated cells. Because ALI5 and ALI14 have been mapped to different regions of PLCγ, we generated PLCγ1 and PLCγ2 variants that incorporated gain-of-function mutations in both regions. A combination of ALI5 and ALI14 mutations in PLCγ2 had a marked affect on basal activity as well as on the level of activation by Rac2 (Fig. 6*A*) or EGF (Fig. 6*B*). The basal activity of this PLCγ2 double mutant was comparable to the PLC activity of the wild-type PLCγ2 in stimulated cells. Similarly, the combination of D1019L and Y509A/F510A mutations in PLCγ1 generated a constitutively active enzyme (Fig. 6*C*).

Previous studies of PLCγ1 that identified the importance of Tyr-509 and Phe-510 residues in the spPH domain also suggested that this replacement bypasses the need for phosphorylation of residues Tyr-775 and Tyr-783 (in the SH2/SH3 linker) required for the activation mediated by receptor and non-receptor tyrosine kinases (30). We therefore tested both the ALI5-type mutation (D1019L) and the Y509A/F510A mutations in the spPH domain in combination with the Y775F/Y783F mutations (Fig. 6). Y775F/Y783F mutations, when introduced into the wild-type PLCγ1, completely blocked responses to EGF (Fig. 6*D*). Interestingly, the activation level of the PLCγ1 variant incorporating D1019L/Y775F/Y783F mutations was much lower than the activation of the D1019L variant (Fig. 6*D*, *left panel*). This suggests that ALI5-type mutations in the ridge region of the catalytic domain enhanced activation dependent on tyrosine phosphorylation and changes in the PLCγ-specific region, the γSA. By contrast, the PLCγ1 Y509A/F510A/Y775F/Y783F variant combining replacements in the spPH domain and sites of tyrosine phosphorylation, both in the γSA, had a similar activation level as the spPH domain mutation alone (Fig. 6*D*, *right panel*); this finding is consistent with previously reported observations (30). Based on data in Fig. 6*D*, *right panel*, it is likely that the gain-of-function replacements in the spPH domain have resulted in changes in the γSA that to some degree overlap with the changes resulting from phosphorylation of Tyr-775 and Tyr-783 residues.

DISCUSSION

Analyses of two mouse strains (ALI5 and ALI14) generated by genome-wide ENU mutagenesis have linked gain-of-function mutations in PLCγ2 to spontaneous inflammation and autoimmunity. An important aspect of the data presented here, obtained from extensive characterization of the PLCγ gain-of-function variants, is their mechanistic implication. Interpretation of the mechanisms that result in gain-of-function is, however, limited by our current lack of knowledge of the PLCγ structure. Despite the progress in solving structures of individual domains from the γSA (20, 31–33), structures of the full-length protein or larger multidomain arrays are lacking. There are, nevertheless, a considerable number of data from mutational analyses of PLCγ enzymes (reviewed in Refs. 34, 35) and more extensive structural information for PLCδ and PLCβ families (36, 37). Based on this information we can con-

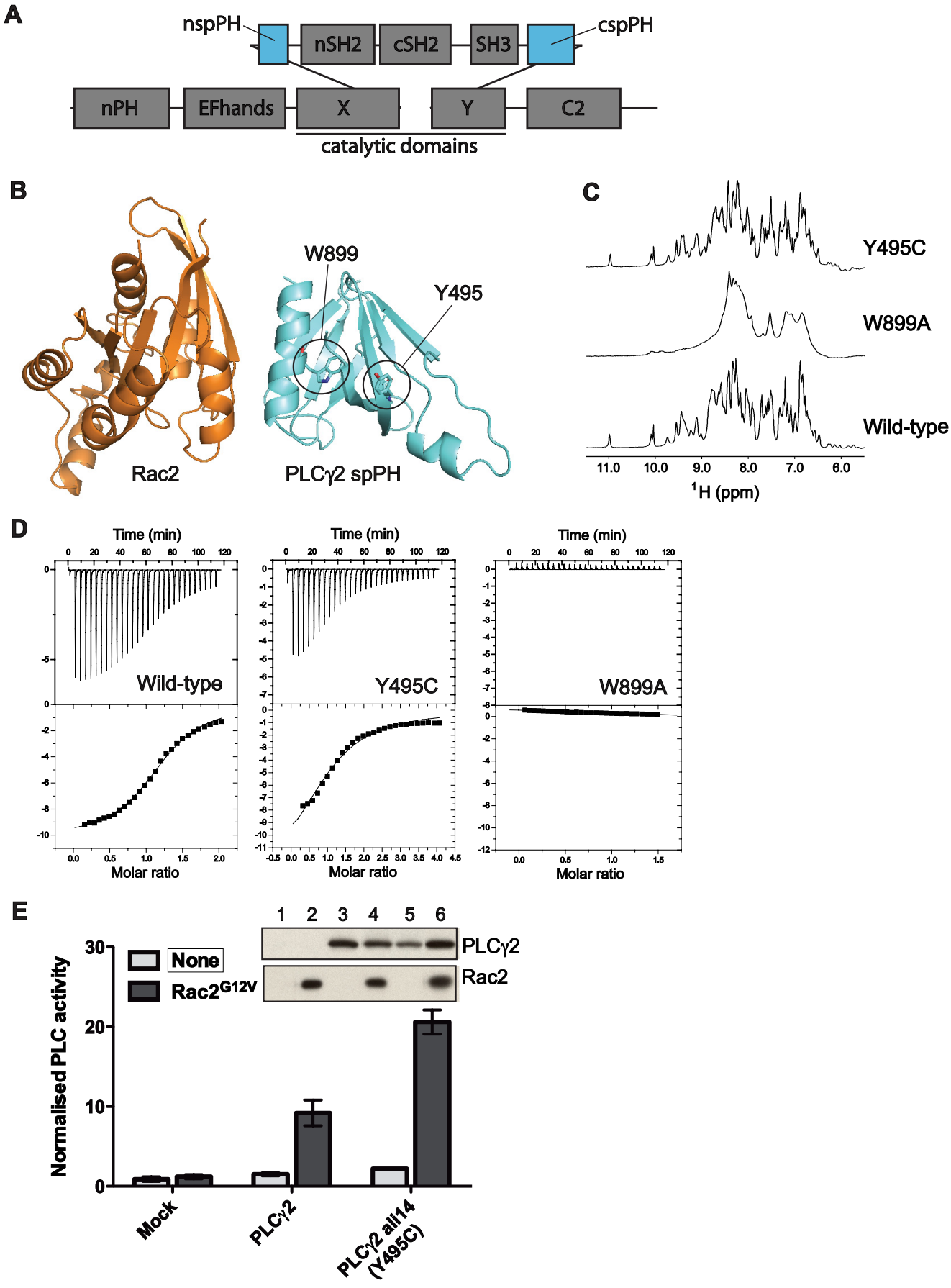
A
nspPH
nSH2
cSH2
SH3
cspPH
nPH
EFhands
X
Y
C2
catalytic domains
B
W899
Y495
Rac2
PLCγ2 spPH
C
Y495C
W899A
Wild-type
11.0
10.0
9.0
8.0
7.0
6.0
^{1}H (ppm)
D
Time (min)
Wild-type
Y495C
W899A
Molar ratio
E
1 2 3 4 5 6
PLCγ2
Rac2
None
Rac2^{G12V}
Normalised PLC activity
30
20
10
0
Mock
PLCγ2
PLCγ2 ali14 (Y495C)

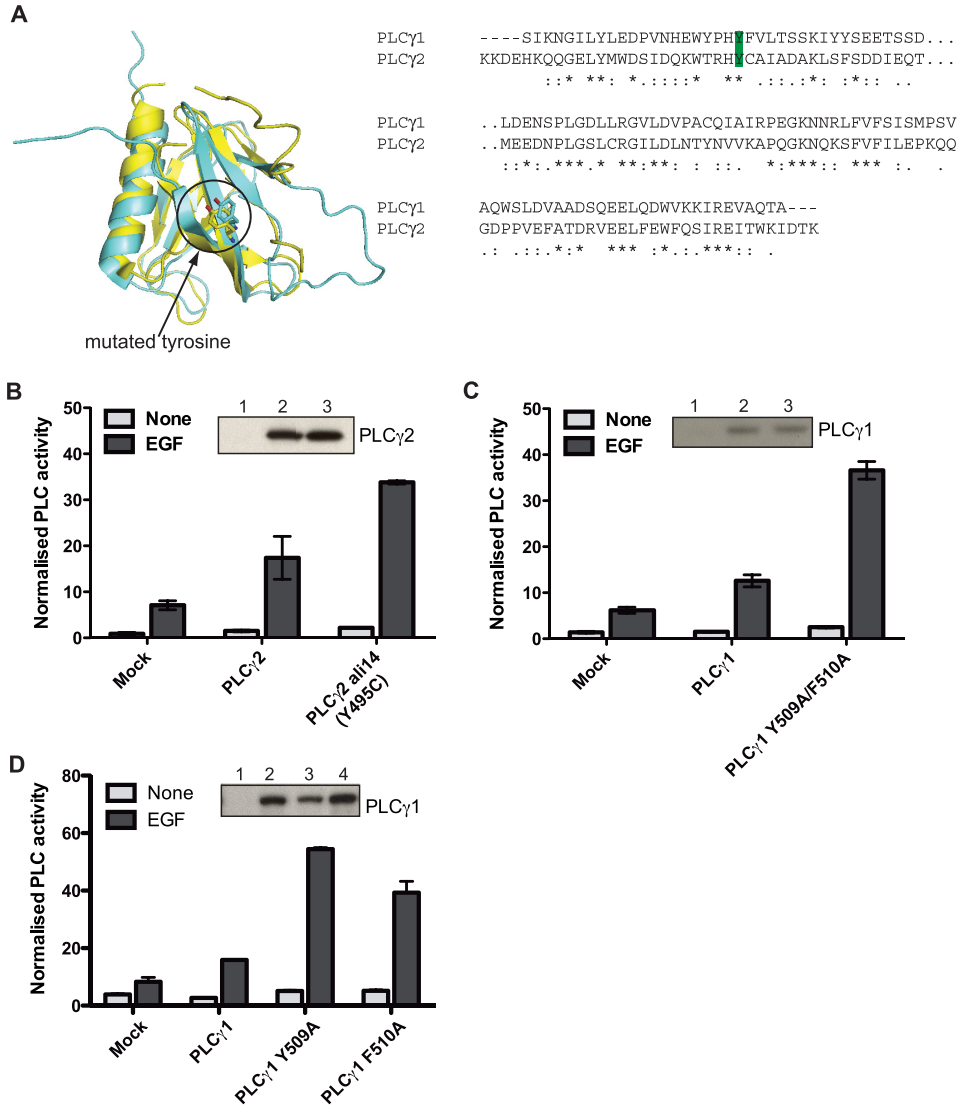

FIGURE 5. **The ALI14 mutation can be transferred into PLCγ1.** *A*, structural alignment (a backbone root mean square difference of 2. 9 Å over 65 core region C atoms) (*left panel*) and sequence alignment (*right panel*) of the PLCγ1 and PLCγ2 spPH domains show that the tyrosine mutated in ALI14 is conserved. *B–D*, PLC activity in transfected COS-7 cells was measured for: (*B*) PLCγ2 wild type and ALI14, (*C*) PLCγ1 wild type and Y509A/F510A variant, and (*D*) PLCγ1 wild type, Y509A, and F510A variants. Inositol phosphate production was measured in nonstimulated COS-7 cells and following stimulation with 100 ng/ml EGF. Protein expression was analyzed by Western blotting (*insets*). *Lanes 1–3* in *B* correspond to mock (*1*), PLCγ2 wild type (*2*), and ALI14 (*3*). *Lanes 1–3* in *C* correspond to mock (*1*), PLCγ1 wild type (*2*), and Y509A/F510A variant (*3*). *Lanes 1–4* in *D* correspond to mock (*1*), PLCγ1 wild type (*2*) Y509A variant (*3*), and F510A variant (*4*). The data in *panels B–D* are representative for at least three independent experiments.

sider possible models and frameworks for interpretation of our findings.

The analysis of the ALI5 mutation in the catalytic domain that is highly conserved in all PLC families (Figs. 1, 2, and 3) suggests that one consequence of the replacement of this negatively charged residue is facilitated membrane interaction of the PLCγ in its activated form, following EGF stimulation or binding to Rac. Consistent with this are previous findings identifying the ridge region, to which the ALI5 mutation has been mapped, as a region interacting with and penetrating the membrane surface (23, 36). However, it is not clear whether or not this region and the adjacent active site could be occluded by other structural elements under basal conditions, rather than being exposed and available for membrane interaction as in the activated enzyme. Recent work on PLCβ2 has shown that some residues within the ridge region are in the vicinity of the loop that connects two parts of the catalytic domain and limits substrate access to the active site (38). Interaction between the ridge region and the loop could therefore contribute to autoinhibition. If similar arrangements are present in PLCγ then the ALI5 replacements could also, to some degree, reduce these inhibitory constraints and thus facilitate the activation process triggered by an interaction with regulatory molecules.

The ALI14 mutation is present in the spPH domain that is itself a site of other regulatory interactions; most notably in PLCγ2 the spPH domain is the binding site for Rac (20). The relative position of the spPH domain to other domains within the γSA or the catalytic domain has not been defined structurally. Several possible interactions, that require further verification, have been suggested by mutational analysis; for example, recent analysis of PLCγ1 suggested that the N-terminal part of the spPH domain could be involved in interaction with the

FIGURE 4. **The ALI14 mutation in the PLCγ2 spPH domain increases activity but does not influence folding or Rac binding.** *A*, diagram indicating the domains of PLCγ. The spPH domain is shown in *blue*. *B*, crystal structure of the complex formed by Rac2 and the spPH domain (Phe-495 variant) (PDB: 2W2X). The position of Tyr-495, present in the sequence of the wild-type PLCγ2 and replaced by cysteine in ALI14, is indicated in the structure of the PLCγ2 spPH domain; the location of Tyr-495 is away from the Rac binding surface. Also indicated is Trp-899. Mutation of this residue to alanine prevents folding of the spPH domain. *C*, one-dimensional ^{1}H NMR spectroscopy was carried out using the isolated spPH domain of PLCγ2. The downfield region encompassing resonances from the backbone NH and aromatic side chain CH protons is depicted for each variant. The maintenance of the narrow linewidths and overall resonance dispersion indicates that ALI14 adopts a globular structure highly similar to the wild type while the broad lines and limited dispersion for PLCγ2 spPH W899A indicates that it is an unfolded protein. *D*, ITC measurements of Rac2 binding were carried out using isolated PLCγ2 spPH; wild type and the spPH variants incorporating ALI14 or W899A mutation were analyzed. For the wild-type spPH domain, the K_d value was 18.5 μM, for ALI14 56.2 μM and for W899A there was no binding. *E*, inositol phosphate production was measured in COS-7 cells transfected with PLCγ2 wild type or ALI14 variant in the presence or absence of Rac2^{G12V}. Protein expression was analyzed by Western blotting (*insets*). *Lanes 1–6* correspond to mock (*1*, *2*), PLCγ2 wild type (*3*, *4*), and ALI14 (*5*, *6*). The data are representative for four independent experiments.

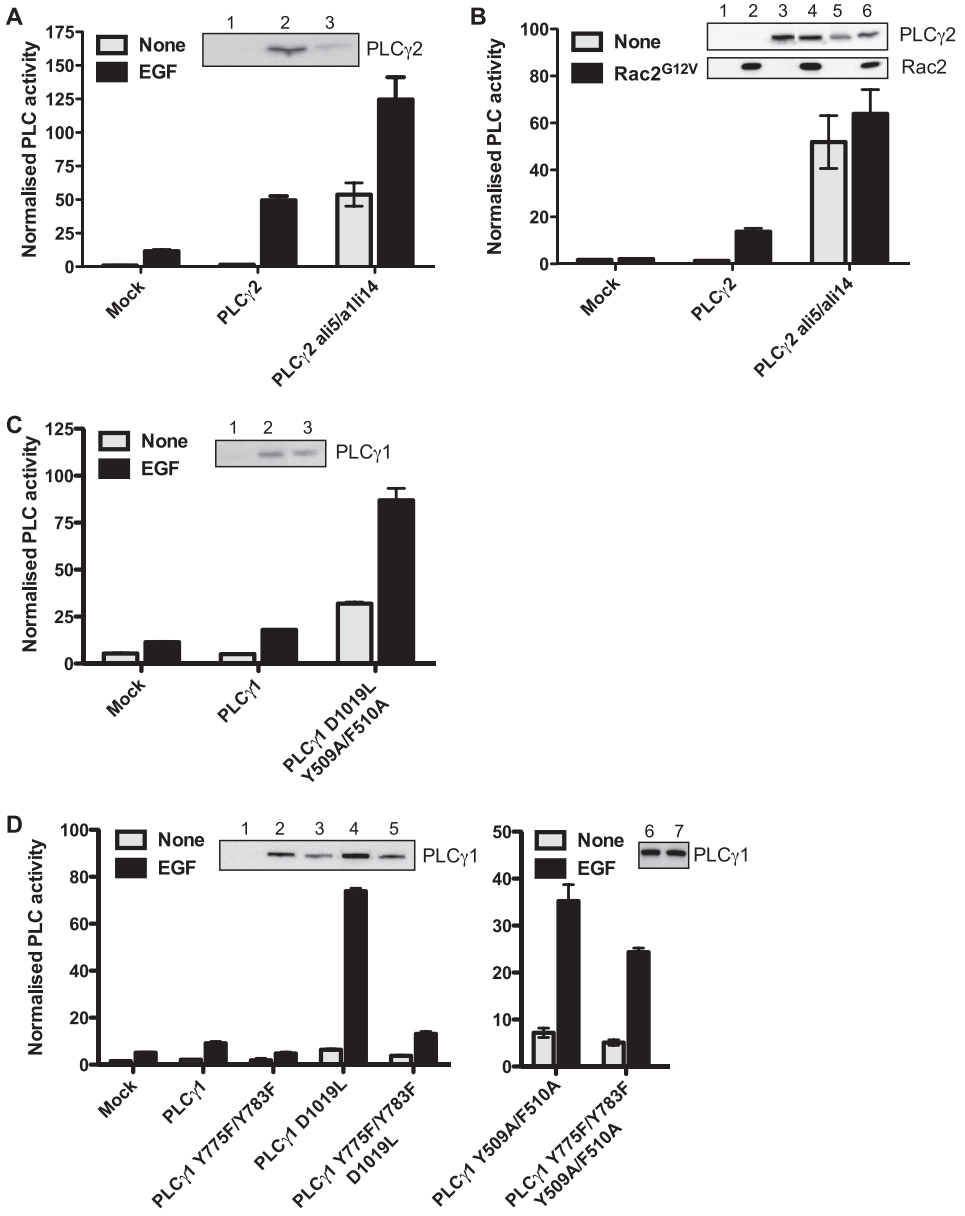

FIGURE 6. **Gain-of-function mutants can be combined to increase basal PLC activity.** Inositol phosphate production was measured in COS-7 cells transiently transfected with the following variants of PLCγ isoforms: (*A*) PLCγ2 wild type and ALI5/ALI14, (*B*) PLCγ2 wild type and ALI5/ALI14, co-transfected with $Rac2^{G12V}$, (*C*) PLCγ1 wild type and D1019L/Y509A/F510A, (*D*) PLCγ1 wild type, Y775F/Y783F, D1019L, Y775F/Y783F/D1019L, Y509A/F510A, and Y775F/783F/Y509A/F510A. Cells were stimulated with 100 ng/ml EGF as indicated. Protein expression was analyzed by Western blotting (*insets*); the expression level of the PLCγ2 ALI5/ALI14 double mutant was consistently lower than the wild type despite the higher activity. *Lanes 1–3* in *A* correspond to mock (*1*), PLCγ2 wild type (*2*), and ALI5/ALI14 (*3*). *Lanes 1–6* in *B* correspond to mock (*1*, *2*), PLCγ2 wild type (*3*, *4*), and ALI5/ALI14 (*5*, *6*). *Lanes 1–3* in *C* correspond to mock (*1*), PLCγ1 wild type (*2*), and D1019L/Y509A/F510A variant (*3*). *Lanes 1–7* in *D* correspond to mock (*1*), PLCγ1 wild type (*2*), Y775F/Y783F variant (*3*), D1019L variant (*4*), Y775F/783F/D1019L variant (*5*), Y509A/F510A variant (*6*), and Y775F/783F/Y509A/F510A variant (*7*). The data are representative for at least three independent experiments.

C-SH2 domain (30). Regardless of the domain organization within the γSA, several lines of experimental evidence suggest that it contains elements involved in autoinhibition (34). In other PLC families the position of the γSA is occupied by shorter (mainly unstructured) linkers connecting the two parts of the catalytic domain. As discussed above for PLCβ2, this region has an inhibitory impact on PLC activity. Similarly, the deletion of the linker region in PLCδ or PLCε enzyme enhances activity (38). Based on our data from analysis of ALI14-type mutations (Figs. 4 and 5) and findings by others (30), it is likely that the spPH domain, including the region with the ALI14 residue, contributes directly or indirectly to formation and/or positioning of surfaces with a role analogous to the PLCβ2 inhibitory loop. It is also likely that different regulatory inputs lead to release of these inhibitory impacts and that ALI14-type mutations could mimic some of the changes brought about by interaction with regulatory molecules. This is illustrated by the finding that ALI14-type mutations bypass requirement for phosphorylation of tyrosine residues required for activation by EGF receptor (Fig. 6).

The finding that ALI5 and ALI14 mutations on their own do not greatly increase basal activity (Fig. 6) is not surprising considering that mutations were introduced in the germ line by ENU mutagenesis and that very potent activating mutations in the germ line could be incompatible with survival (21). ALI5 and ALI14 mutations, in the ridge region of the catalytic domain and in the spPH domain of the γSA, cooperate to generate a constitutively active enzyme (Fig. 6) supporting their distinct impact on the regulatory mechanism.

Based on all these considerations, we propose a model suggesting that each mutation could destabilize, but not overcome, autoinhibition in the inactive form of the enzyme facilitating different steps of the activation mechanism; in addition, ALI5-type mutations could enhance membrane interaction in the active state. These insights extend our understanding of molecular mechanisms that regulate activity of PLCγ enzymes and support the concept that their aberrant signaling can be a consequence of point mutations that affect these mechanisms.

Acknowledgments—We thank B. Rellahan and P. Gierschik for constructs of PLCγ1 and Rac2.

REFERENCES

1. Suh, P. G., Park, J. I., Manzoli, L., Cocco, L., Peak, J. C., Katan, M., Fukami, K., Kataoka, T., Yun, S., and Ryu, S. H. (2008) *BMB Rep.* **41,** 415–434

2. Drin, G., and Scarlata, S. (2007) *Cell Signal.* **19,** 1383–1392
3. Bunney, T. D., and Katan, M. (2006) *Trends Cell Biol.* **16,** 640–648
4. Katan, M. (2005) *Biochem. J.* **391,** e7–9
5. Ji, Q. S., Winnier, G. E., Niswender, K. D., Horstman, D., Wisdom, R., Magnuson, M. A., and Carpenter, G. (1997) *Proc. Natl. Acad. Sci. U.S.A.* **94,** 2999–3003
6. Wang, D., Feng, J., Wen, R., Marine, J. C., Sangster, M. Y., Parganas, E., Hoffmeyer, A., Jackson, C. W., Cleveland, J. L., Murray, P. J., and Ihle, J. N. (2000) *Immunity* **13,** 25–35
7. Wells, A. (2000) *Adv. Cancer Res.* **78,** 31–101
8. Jones, N. P., and Katan, M. (2007) *Mol. Cell. Biol.* **27,** 5790–5805
9. Jones, N. P., Peak, J., Brader, S., Eccles, S. A., and Katan, M. (2005) *J. Cell Sci.* **118,** 2695–2706
10. van Rheenen, J., Song, X., van Roosmalen, W., Cammer, M., Chen, X., Desmarais, V., Yip, S. C., Backer, J. M., Eddy, R. J., and Condeelis, J. S. (2007) *J. Cell Biol.* **179,** 1247–1259
11. Sala, G., Dituri, F., Raimondi, C., Previdi, S., Maffucci, T., Mazzoletti, M., Rossi, C., Iezzi, M., Lattanzio, R., Piantelli, M., Iacobelli, S., Broggini, M., and Falasca, M. (2008) *Cancer Res.* **68,** 10187–10196
12. Guo, S., Ferl, G. Z., Deora, R., Riedinger, M., Yin, S., Kerwin, J. L., Loo, J. A., and Witte, O. N. (2004) *Proc. Natl. Acad. Sci. U.S.A.* **101,** 14180–14185
13. Yu, P., Constien, R., Dear, N., Katan, M., Hanke, P., Bunney, T. D., Kunder, S., Quintanilla-Martinez, L., Huffstadt, U., Schröder, A., Jones, N. P., Peters, T., Fuchs, H., Hrabé, de, Angelis, M., Nehls, M., Grosse, J., Wabnitz, P., Meyer, T. P., Yasuda, K., Schiemann, M., Schneider-Fresenius, C., Jagla, W., Russ, A., Popp, A., Josephs, M., Marquardt, A., Laufs, J., Schmittwolf, C., Wagner, H., Pfeffer, K., and Mudde, G. C. (2005) *Immunity* **22,** 451–465
14. de Gorter, D. J., Beuling, E. A., Kersseboom, R., Middendorp, S., van Gils, J. M., Hendriks, R. W., Pals, S. T., and Spaargaren, M. (2007) *Immunity* **26,** 93–104
15. Arteaga, C. L., Johnson, M. D., Todderud, G., Coffey, R. J., Carpenter, G., and Page, D. L. (1991) *Proc. Natl. Acad. Sci. U.S.A.* **88,** 10435–10439
16. Nomoto, K., Tomita, N., Miyake, M., Xhu, D. B., LoGerfo, P. R., and Weinstein, I. B. (1995) *Mol. Carcinog.* **12,** 146–152
17. Poulin, B., Sekiya, F., and Rhee, S. G. (2005) *Proc. Natl. Acad. Sci. U.S.A.* **102,** 4276–4281
18. Sekiya, F., Poulin, B., Kim, Y. J., and Rhee, S. G. (2004) *J. Biol. Chem.* **279,** 32181–32190
19. Piechulek, T., Rehlen, T., Walliser, C., Vatter, P., Moepps, B., and Gierschik, P. (2005) *J. Biol. Chem.* **280,** 38923–38931
20. Walliser, C., Retlich, M., Harris, R., Everett, K. L., Josephs, M. B., Vatter, P., Esposito, D., Driscoll, P. C., Katan, M., Gierschik, P., and Bunney, T. D. (2008) *J. Biol. Chem.* **283,** 30351–30362
21. Hrabé, de, Angelis, M., Flaswinkel, H., Fuchs, H., Rathkolb, B., Soewarto, D., Marschall, S., Heffner, S., Pargent, W., Wuensch, K., Jung, M., Reis, A., Richter, T., Alessandrini, F., Jakob, T., Fuchs, E., Kolb, H., Kremmer, E., Schaeble, K., Rollinski, B., Roscher, A., Peters, C., Meitinger, T., Strom, T., Steckler, T., Holsboer, F., Klopstock, T., Gekeler, F., Schindewolf, C., Jung, T., Avraham, K., Behrendt, H., Ring, J., Zimmer, A., Schughart, K., Pfeffer, K., Wolf, E., and Balling, R. (2000) *Nat. Genet.* **25,** 444–447
22. Fuchs, H., Schughart, K., Wolf, E., Balling, R., and Hrabé, de, Angelis, M. (2000) *Mamm. Genome* **11,** 528–530
23. Ellis, M. V., James, S. R., Perisic, O., Downes, C. P., Williams, R. L., and Katan, M. (1998) *J. Biol. Chem.* **273,** 11650–11659
24. Bunney, T. D., Opaleye, O., Roe, S. M., Vatter, P., Baxendale, R. W., Walliser, C., Everett, K. L., Josephs, M. B., Christow, C., Rodrigues-Lima, F., Gierschik, P., Pearl, L. H., and Katan, M. (2009) *Mol. Cell* **34,** 223–233
25. Bordoli, L., Kiefer, F., Arnold, K., Benkert, P., Battey, J., and Schwede, T. (2009) *Nat. Protoc.* **4,** 1–13
26. Dunbrack, R. L., Jr. (1999) *Proteins Suppl.* **3,** 81–87
27. Laskowski, R. A., Rullmannn, J. A., MacArthur, M. W., Kaptein, R., and Thornton, J. M. (1996) *J. Biomol. NMR* **8,** 477–486
28. Wiederstein, M., and Sippl, M. J. (2007) *Nucleic Acids Res.* **35,** W407–410
29. Stahelin, R. V., and Cho, W. (2001) *Biochemistry* **40,** 4672–4678
30. DeBell, K., Graham, L., Reischl, I., Serrano, C., Bonvini, E., and Rellahan, B. (2007) *Mol. Cell. Biol.* **27,** 854–863
31. Pascal, S. M., Singer, A. U., Gish, G., Yamazaki, T., Shoelson, S. E., Pawson, T., Kay, L. E., and Forman-Kay, J. D. (1994) *Cell* **77,** 461–472
32. Kohda, D., Hatanaka, H., Odaka, M., Mandiyan, V., Ullrich, A., Schlessinger, J., and Inagaki, F. (1993) *Cell* **72,** 953–960
33. Wen, W., Yan, J., and Zhang, M. (2006) *J. Biol. Chem.* **281,** 12060–12068
34. Carpenter, G., and Ji, Q. (1999) *Exp. Cell Res.* **253,** 15–24
35. Katan, M., Rodriguez, R., Matsuda, M., Newbatt, Y. M., and Aherne, G. W. (2003) *Adv. Enzyme Regul.* **43,** 77–85
36. Essen, L. O., Perisic, O., Cheung, R., Katan, M., and Williams, R. L. (1996) *Nature* **380,** 595–602
37. Jezyk, M. R., Snyder, J. T., Gershberg, S., Worthylake, D. K., Harden, T. K., and Sondek, J. (2006) *Nat. Struct. Mol. Biol.* **13,** 1135–1140
38. Hicks, S. N., Jezyk, M. R., Gershburg, S., Seifert, J. P., Harden, T. K., and Sondek, J. (2008) *Mol. Cell* **31,** 383–394